Conf-9505155--2

SAND94-2059C

Development of a 75-kW Heat-Pipe Receiver for Solar Heat-Engines

Douglas R. Adkins, Charles E. Andraka, and Timothy A. Moss
Sandia National Laboratories, Albuquerque, NM
(505) 844-0611

Abstract

A program is now underway to develop commercial power conversion systems that use parabolic dish mirrors in conjunction with Stirling engines to convert solar energy to electric power. In early prototypes, the solar concentrator focused light directly on the heater tubes of the Stirling engine. Liquid-metal heat-pipes are now being developed to transfer energy from the focus of the solar concentrator to the heater tubes of the engine. The dome-shaped heat-pipe receivers are approximately one-half meters in diameter and up to 77-kW of concentrated solar energy is delivered to the absorber surface.

Over the past several years, Sandia National Laboratories, through the sponsorship of the Department of Energy, has conducted a major program to explore receiver designs and identify suitable wick materials. A high-flux bench-scale system has been developed to test candidate wick designs, and full-scale systems have been tested on an 11-meter test-bed solar concentrator. Procedures have also been developed in this program to measure the properties of wick materials, and an extensive data-base on wick materials for high temperature heat pipes has been developed. This paper provides an overview of the receiver development program and results from some of the many heat-pipe tests.

INTRODUCTION

Dish-Stirling systems integrate a parabolic-dish mirror with one or more Stirling engine/generators to convert solar energy to electrical power. In 1984, the Advanco-Vanguard dish-Stirling module demonstrated a world record peak efficiency of 29.4% for sunlight to electrical power conversion (Washom, 1984). McDonnell Douglas Corp. further developed this technology with six, 25-kW systems fielded around the country (Coleman and Raetz, 1986).

In both the Advanco and the McDonnell Douglas systems, the concentrated solar energy was focused directly on the heater tubes of the Stirling engines. Direct illumination of the tubes created high stress areas that limited the life of the solar receiver. With direct illumination, it was also difficult to provide a balanced power input to each cycle of multi-cylinder engines.

Heat-pipe receivers were conceived as an improvement over the directly illuminated tube receivers. With a heat-pipe receiver, concentrated solar energy heats a dome-shaped absorber surface (see Figure 1), and liquid sodium in the heat pipe removes the heat as it evaporates away. Energy is transferred to the working fluid of the Stirling engine as the sodium vapor condenses. Liquid sodium then flows back to the evaporator surface where it is distributed across the surface by the capillary-pumping action of a wick.

Sandia has been conducting a dish-Stirling receiver development program to support design, development and testing of the heat-pipe receiver concept. Through joint-venture commercialization programs with industry (Cummins Power Generation and Science Applications International Corporation), the Department of Energy has promoted the use of demonstrated technology in dish-Stirling systems.

DISCLAIMER

DISCLAIMER

Sandia and the National Renewable Energy Laboratory have also continued development of advanced heat pipe receiver technologies.

Cummins Power Generation is currently developing 7.5 kW_e dish-Stirling systems that will require a 35 kW_t heat-pipe receiver. A receiver developed for this system by Thermacore Incorporated was tested on-sun at Sandia at a power throughput of 56 kW_t (this limit was a function of the test equipment and the insolation, not the receiver). This receiver has subsequently undergone testing on a lamp assembly at Thermocore for over 2500 hours with frequent freeze-thaw cycles. More recently, Thermacore improved the permeability of their wick powder and built a receiver with a design power throughput of 120 kW_t. The demonstrated throughput of this receiver was 65 kW_t. (Once again, this was a limit of the test equipment and not the receiver.)

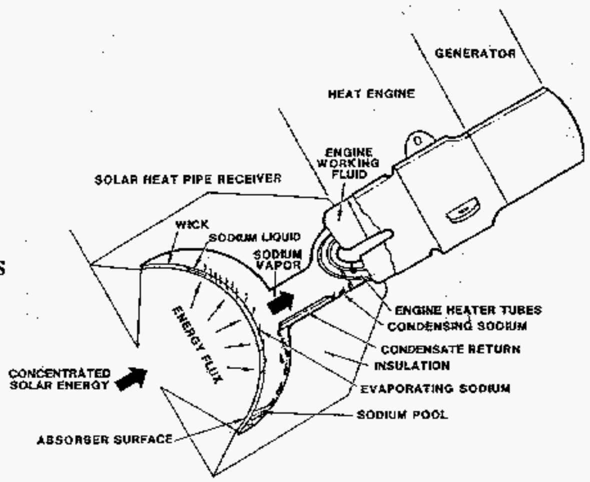

Figure 1. Operation of a heat-pipe solar. receiver

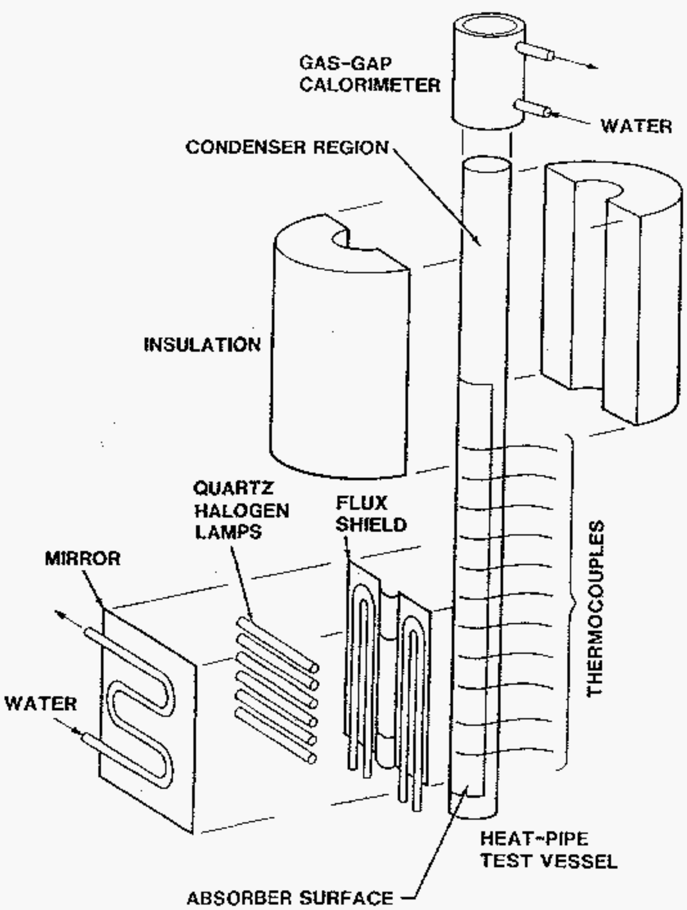

Figure 2. Test system for bench-scale heat-pipe receivers.

To compliment the work by Cummins and Thermacore, Sandia is exploring a wide-range of wick materials through property measurements, performance models, and bench-scale and full-scale tests. High-flux tests with bench-scale receiver systems are conducted to establish the performance and durability of various wick structures, and to avoid the trouble and cost of full-scale receiver tests. The test system for the bench-scale heat-pipe receivers is illustrated in Figure 2. A lamp array with either six or twelve quartz halogen bulbs is focused on the test section of the heat pipe and the power is increased until over-temperature conditions are observed with thermocouples mounted on the heated surface. The operating temperature of the pipe is controlled by a water-cooled calorimeter that is mounted on the top end of the heat pipe. By regulating the ratio of helium to argon that flows between the calorimeter and the heat pipe, the power that is extracted from the pipe can be controlled. The lamps are capable of providing a peak flux of about 68 W/cm^2 to the surface of the heat pipe, and the lamp assembly can be placed at increasingly higher elevations along the pipe to force liquid to flow further through the wick structure against gravity.

Once the performance of a wick structure is demonstrated in bench-scale tests, a full-scale system is constructed and tested on the sun to determine the limits of the system, and examine the effects of orientation and operating conditions. Full-scale receivers are tested on a parabolic mirror solar concentrator at Sandia National Laboratories. The Test Bed Concentrator (TBC) is an 11-m dish that tracks the sun on an azimuth-elevation tracking system. On a day with 1000 W/m^2 insolation levels, it can deliver approximately 77 kW of power through an 20.3-cm circular aperture. Energy is removed from the receiver either by gas-gap calorimeters or Stirling engines. A solar-blind infrared (IR) camera near the vertex of the dish mirror is used to monitor the temperatures across the surface of the receiver.

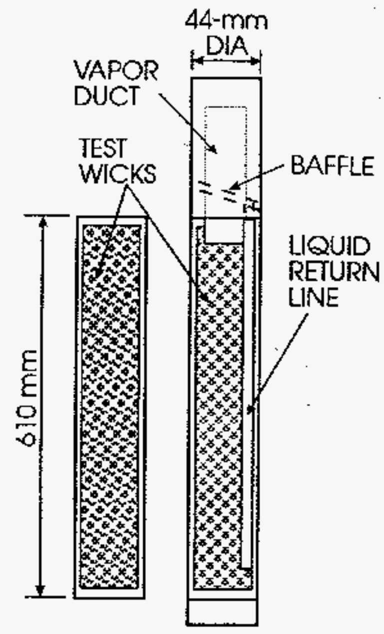

Figure 3. Internal design of bench-scale heat-pipe receivers

BENCH-SCALE TESTS

A series of bench-scale heat-pipe receiver tests have been conducted to study the performance of various wick materials and artery structures. Figure 3 illustrates a typical internal configuration of the bench-scale systems. The wick structure on the inner surface of the heat pipe transports the liquid up to the region that is heated by the lamps. To prevent liquid from flowing directly onto the wick structure, a gutter system in the condenser diverts liquid directly to the pool at the bottom of the pipe. The gutter insures that all liquid reaching the heated region is forced to flow from the pool and through the wick structure. The vapor duct in the center of the condenser prevents liquid from being entrained and swept into the condenser.

Based on current designs, a full-scale 75-kW$_t$ solar receiver will be on the order of 0.4-0.5 meters in diameter. For capillary pumping to meet hydrostatic pressure requirements alone, the effective pore radius at the top of the receiver must be less than 75 μm. When pressure drops associated with the flux loading are added to the hydrostatic requirements, a 1-cm thick wick with a Darcy permeability of 150 μm^2 would require an effective pore radius of 40 μm or less to properly cool the receiver [Adkins, 1990]. These performance standards are well beyond the capabilities of most wick materials, so the designer is left with the prospect of using an extensive artery structure, or including an electromagnetic pump in the system. Neither option is attractive for reliability reasons. Gravity feed systems are considered unreliable because momentary interruptions by clouds can cause full-power restarts with an inadequate liquid supply.

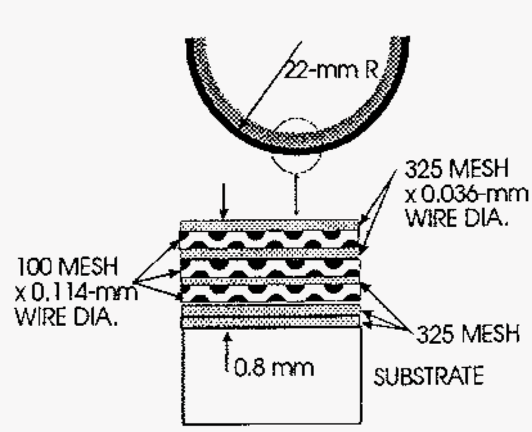

Figure 4. Composite screen wick structure.

One of the wicks tested in the bench-scale system was a composite structure with alternating layers of 100 mesh and 325-mesh stainless steel screens sintered to the inner surface of a stainless steel tube (see Figure 4). The effective pore radius of a 100-mesh screen is on the order of 130 μm when measured perpendicular to the wick surface. In a stacked composition, however, the effective pore radius is more like half the wire diameter. The effective pore radius for the composite wick shown in Figure 4 was measured to be 51 μm and the permeability was 81 μm^2. Screens in the composite wick were sinter bonded in a hydrogen oven for two hours at 1050°C. The final thickness was 0.8 mm.

After vacuum bake-out and fill operations, high-flux tests were conducted on the composite wick structure with a 12-bulb lamp array. The quartz-lamp array delivers an average flux of about 60 W/cm^2 to a 3.4-cm x 20-cm vertical strip along a heat pipe. With the bottom of the heated section at the surface of the pool, stable heat-pipe operation was observed up to flux levels of about 40 W/cm^2. At higher flux levels, there were signs that portions of the heated surface were no longer being cooled by the sodium. Based on the measured properties of the wick, the capillary pumping capabilities of the wick would have been exceeded at flux levels of around 30 W/cm^2. Performance beyond the calculated limit could be attributed to condensation on the wick above the heated region.

Spin-forming and hydro-forming a sintered stack of screens was found to cause an excessive reduction in permeability. To retain the permeability of the wick, it is necessary to first spin-form the screens, and then sinter the screens to the receiver dome. This process of forming a wick, however, was both time consuming and expensive.

With a brazed powder wick, many of the problems associated with applying a screen-wick structure to the evaporator surface could be avoided. In addition to the composite wick tests, a brazed powder wick was tested in the same bench-scale receiver vessel. Friction Coatings in Sterling Heights, MI formed the stainless-steel powder and braze mixture through a proprietary process, and then applied the material to the inner surface of the tube by decalcomania. The wick structure on the tube substrate was then heated in an oven to complete the braze process.

The brazed-powder wick was 0.9-mm thick and the permeability was measured to be approximately 40 μm^2. The measured effective pore radius was 69 μm. Tests with a six-bulb lamp array showed that the wick structure could support a 60 W/cm^2 load over 3.4-cm x 10-cm area. The lamps were placed just above the surface of the liquid in the heat pipe, so hydrostatic pressure drops were minimized. When the twelve-bulb array was used to heat a 3.4-cm x 20-cm patch, it was not possible to achieve stable operation.

Through many iterations in mixing parameters, it was not possible to significantly reduce the effective pore radius without compromising the permeability of the brazed-powder wick. It also proved to be difficult to achieve a thick coating (3 mm or greater) of the brazed-powder material on the entire surface of a receiver dome. The extensive artery structure that would be required for the brazed-powder wick structure made this approach less attractive.

The final wick structure explored in this series of tests was a metal felt fabric produced by Bekaert Fibre Technologies of Belgium. Bekipor® felts are most commonly used in filter applications, and, in an unsintered state, they are flexible enough to easily conform to the shape of a receiver dome. The material is made of fine wires (≈10 μm diameter) that are chopped to short lengths and then laid down to form a high-porosity mat.

Two felt metal wick structures were tested in bench-scale receivers. One wick was made of Bekipor® 4/150 and the other wick used 8/300 felt (the 8 refers to the fiber wire diameter in microns and the 300 refers to the weight of one square meter of the material in grams). A single layer of either felt is about 1-cm thick in an unsintered state, but it compacts easily and the thickness reduces between 30 to 50% during sintering. When compacted to 1-mm thick, the 4/150 felt still has a porosity of 98%, a permeability of

160 μm², and an effective pore radius of approximately 50 μm. A full discussion of felt wick properties and the impact of compacting is given by Adkins et al. [1995].

Figure 5 shows the configuration of the bench-scale receiver for the felt metal wick tests. It was necessary to apply the felt to a convex surface because shrinkage of the wick during sintering made the felt lift off of the concave inner surface of a tube. On one surface, two layers of 4/150 felt were sintered and then compacted to about 5.5-mm thick. Two layers of 8/300 were sintered and compacted to about 5.5-mm thick on the second surface. The fragile nature of the felt made it difficult to measure the permeability and pore size directly on the fabricated wick. Based on the final thickness of the 4/150 wick, however, the permeability would be on the order of 600 μm², and about 70% of the pores would have an effective radius of 60 μm or smaller. The 8/300 also has a permeability of about 600 μm², but the effective pore radius was estimated to be larger than 100 μm.

With the lamps located near the top of the wick, the heat pipe was capable of withstanding a full power startup with an initial surface temperature just above the sodium melting temperature. The total power throughput was 4200 W, so the average flux over the 3.4-cm x 20-cm heated surface was approximately 62 W/cm². In these tests, liquid sodium was required to travel about 40 cm through the wick to cool the top of the heated region. No problems were encountered with the 4/150 wick system, and the system operation was limited by the power of the lamp array.

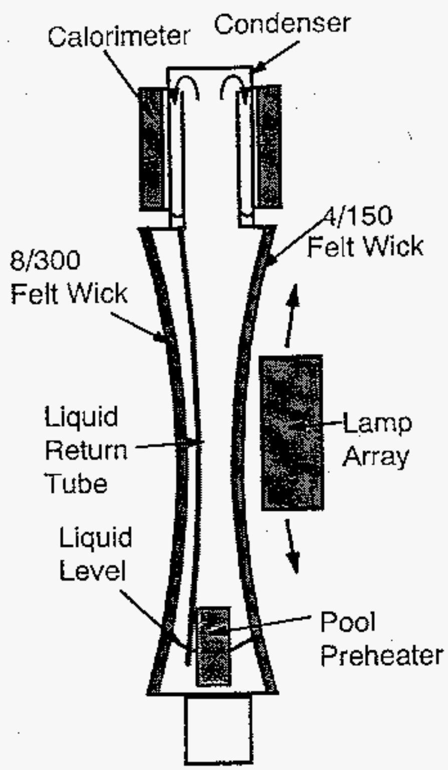

Figure 5. Configuration of the bench-scale heat-pipe receiver with a felt-metal wick.

The 8/300 felt metal wick performed poorly in the bench-scale heat pipe tests. At an average flux level of about 30 W/cm², the surface overheated just below the top of the heated region. The overheating problem resurfaced at even lower levels on restarting. This phenomena was repeated when the lamps were moved down the heat pipe to a new location. After the heat pipe was disassembled, it was found that the sintered bond between the 8/300 and the substrate material was weak in several areas. The sintered bond between the 4/150 and the substrate appeared to be uniformly good. Sintering on both materials was performed simultaneously in a hydrogen oven at 1050°C for two hours. It was postulated that the fine diameter of the 4/150 wires allowed the material to conform better to the substrate surface.

FULL-SCALE TESTS

From the bench-scale receiver tests, it appeared that the Bekipor® 4/150 felt would perform better in a full-scale solar receiver than any other wick material. A wick-covered dome for the full-scale receiver was produced by Porous Metal Products in Jacksboro, Texas, and the felt was provided by Bekaert Corporation in Marietta, GA. The 41.5-cm diameter hemispherical dome was covered with two layers of the 4/150 felt.

It was necessary to use seams in both layers of felt because of the depth of the full hemisphere dome. The seams were made along four radial paths extending about 20 cm in from the edge, and the seams were staggered between the layers.

After sintering, the wick was 2.5 to 2.8 mm thick near the center of the dome, and between 3.3 to 4.3-mm thick towards the edge. The measured permeability near the top of the dome was 185 μm^2. An effective pore radius could not be determined directly, but, based on the thickness and mercury porosimetry measurements given by Adkins et al. [1995], 70% of the pores would have an effective pore radius of 48 μm or smaller.

Sandia integrated the wick-covered dome into a receiver system. Cummins Power Generation provided the receiver hardware as part of their ongoing effort to develop dish-Stirling power generating systems. Both the receiver dome and the rest of the heat pipe envelope were made of Haynes-230 alloy. As in the bench-scale receiver, a duct ran through the center of the condenser to reverse the vapor flow and drive condensate towards the evaporator. Baffles in the front section of the receiver prevented condensate from flowing directly onto the evaporator surface.

The receiver was vacuum baked at 700°C for 4 days to remove non-condensable gasses and water vapor. A 3190-cc charge of purified liquid sodium was loaded into the receiver. Heaters were mounted on the receiver for melting the sodium and thermocouples were mounted on the back surface for controlling the heaters. Four thermocouples were also spot welded to the front (absorber) surface of the receiver at the 3, 6, 9, and 12 o'clock positions about 6 cm from the edge of the dome. The absorber surface was also monitored by an IR camera mounted at the vertex of the solar concentrator.

The receiver was mounted on a test-bed concentrator at Sandia for performance testing. With the aperture left fully open for IR camera monitoring, the test-bed concentrator can provide a maximum throughput power of about 60 kW. Initially, tests began at sunrise so the power would gradually increase while the receiver came to a setpoint vapor temperature of 725°C. In general, the receiver performed well up to full power. Impending dryout conditions were noted on two occasions.

At temperatures over 400°C, the sodium pool was clearly visible in the IR image as a dark region at the bottom of the receiver. Based on the IR images and volume calculations, the pool was 8-cm deep. The pool image would generally disappear as the receiver reached the set-point temperature and the calorimeters began to draw power. Prior to the pool disappearing, a slight warm area (less than 20°C hotter) appeared above the center of the IR image. The warm area corresponds to a high-flux area where our model predicts initial dryout. We suspect that when the pool dissappears from the IR image, it begins boiling, and bathes the wick with additional liquid. This bathing action seems to improve the system's heat transport capabilities.

A shutter in front of the receiver allowed the system to be subjected to rapid restarts which simulate cloud transients. After several restarts at a 60-kW_t throughput power level, a small but rapidly heating hotspot appeared just below the center of the receiver image. Careful measurement led to the conclusion that the hotspot corresponds to the end of a seam in the wick material where a slight pucker in the felt may have formed. Future receivers will be built without seams in the felt material.

The receiver was also started from a frozen state with a 40 kW incident power level. In these tests, temperatures would rise rapidly to about 400°C, and then slow as evaporative heat transport became more dominant. The receiver reaches 700°C within 7 minutes of going on-sun. At 40 to 50 kW_t throughput, rapid changes in the setpoint temperature and the operating power had no adverse effect on receiver operation. The receiver has since been tested by Cummins Power Generation on a 36 kW_t dish (CPG-460). It routinely operates at a 32 kW_t throughput power level, and it is subjected to daily high-power startups from a frozen state.

Receiver tests with the felt-metal wicks proved the feasibility of heat-pipe solar receivers operating in the power ranges necessary for 25 kW_e Stirling engine systems. Long term durability of these systems remains to be demonstrated. Bench-scale tests have just been completed to examine the impact of freezing and thawing cycles on the felt wick structure. A second bench-scale system is also being constructed to examine the effect of long-term exposure of the felts to a high-temperature sodium environment. Finally, a second full-scale heat-pipe solar receiver will be fabricated to study the operation of the receiver when condensate is allowed to flow directly to the evaporator surface.

CONCLUSIONS

Heat-pipe receivers are an attractive option to interface a solar concentrator with a Stirling engine. Several wick materials have been examined to determine the optimum wick structure for a solar heat-pipe receiver. The options examined included composite screen structures, brazed stainless-steel powders, and sintered stainless-steel felts.

The performance of both the composite screen and brazed powder structures were below the requirements necessary for a 25-kW_e dish-Stirling system. An extensive artery network would be needed if these wick materials were selected. The felt-metal wick structure, however, performed well and the high permeability and high capillary pumping capabilities make it an attractive candidate for large solar receivers.

It was demonstrated that a full-scale receiver with a felt-metal wick structure could reliably transfer 60 kW of thermal power. The tests showed that frozen starts and rapid restarts were possible with this system. Future work will examine the long-term durability of felt-wick structures in high temperature sodium environments.

Acknowledgments

The authors would like to thank Howard Cole of Porous Metal Products and Nicos Andreas of Bekaert Corporation for their assistance and expertise in felt metal materials. This work was supported by the United States Department of Energy under contract DE-AC04-94AL85000. Sandia No. SAND94-2059C

References

Adkins, D. R., "Design Considerations for Heat-Pipe Solar Receivers," J. of Solar Energy Eng., Vol. 112, August 1990, pp. 169-176.

Adkins, D.R., T. A. Moss, C. E. Andraka, H. M. Cole, and N. H. Andreas, "An Examination of Felt Wicks for Heat-Pipe Applications," Proceedings of the 4th ASME/JSME Solar Engineering Joint Conf., Lahaina, Maui, HA, 1995.

Coleman, G. C. and J. E. Raetz, "Field Performance of Dish Stirling Solar Electric Systems," Paper No. 869136, Proceedings of the 21st IECEC, San Diego, CA, 1986.

Washom, B., "Parabolic Dish Stirling Module Development and Test Results," Paper No. 849516, Proceedings of the 19th IECEC, San Francisco, CA, 1984.